

Signature splitting in ^{173}W with triaxial particle rotor model

B. Qi,¹ S.Q. Zhang,^{1,2,*} S.Y. Wang,³ and J. Meng^{1,2,4,5,†}

¹*School of Physics, and State-Key Lab. Nucl. Phys. & Tech.,
Peking University, Beijing 100871, China*

²*Institute of Theoretical Physics, Chinese Academy of Sciences, Beijing, 100080, China*

³*Department of Space Science and Applied Physics,
Shandong University at Weihai, Weihai 264209, China*

⁴*Department of Physics, University of Stellenbosch, Stellenbosch, South Africa*

⁵*Center of Theoretical Nuclear Physics,
National Laboratory of Heavy Ion Accelerator, Lanzhou 730000, China*

Abstract

A particle rotor model with a quasi-neutron coupled with a triaxially deformed rotor is applied to study signature splitting for bands with intruder orbital $\nu 7/2^+[633]$ and non-intruder orbital $\nu 5/2^- [512]$ in ^{173}W . Excellent agreement with the observed energy spectra has been achieved for both bands. Signature splitting for band $\nu 7/2^+[633]$, and band $\nu 5/2^- [512]$ before the onset of signature inversion, is satisfactorily reproduced by introducing the γ degree of freedom. The phase and amplitude of signature splitting in band $\nu 5/2^- [512]$ is attributed to strong competition between $2f_{7/2}$ and $1h_{9/2}$ components. However, the explanation of signature inversion in band $\nu 5/2^- [512]$ self-consistently is beyond the present one quasi-neutron coupled with a triaxially deformed rotor.

PACS numbers: 21.60.Ev, 21.10.Re, 23.20.Lv

keyword: Signature splitting, ^{173}W , triaxial deformation, particle rotor model

*sqzhang@pku.edu.cn

†mengji@pku.edu.cn

I. INTRODUCTION

Signature splitting in rotational bands, and especially signature inversion, has attracted much attention for decades. Signature α is a quantum number describing the symmetry associated with the rotation of 180° about one of the three principal axes. The spin sequences for a band with signature α are $I = \alpha + 2n$ ($n = 0, 1, \dots$), with $\alpha = 0$ or 1 in even-mass nuclei and $\alpha = \pm\frac{1}{2}$ in odd-mass nuclei. In general, signature partner bands are not energetically equivalent. One band is favored, i.e., lower in energy, whereas the other one is separated by the so-called signature splitting, which is due to the Coriolis interaction. Signature splitting is usually characterized by $S(I) = [E(I) - E(I - 1)] - \frac{1}{2}[E(I + 1) - E(I) + E(I - 1) - E(I - 2)]$, which appears as a typical staggering curve. An interesting phenomenon is that in several cases the energetically favored and unfavored signature bands may cross each other and interchange their role, i.e., the signature splitting changes its staggering phase with spin I . This phenomenon is known as signature inversion [1]. For the configuration of one-quasiparticle (1-qp) in high- j orbitals, the favored signature is obtained by a simple rule $\alpha_f = (-1)^{j-1/2}\frac{1}{2}$ [2]. However, for a 2-qp configuration in odd-odd nuclei, the expectative favor band with $\alpha_f = (-1)^{j_p-1/2}\frac{1}{2} + (-1)^{j_n-1/2}\frac{1}{2}$ may become energetically unfavored. Similar effects have been also observed for some 3-qp bands in odd- A nuclei. One may also refer to such phenomenon as signature inversion.

Signature inversions have been observed systematically in regions of mass number $A \sim 80$, $A \sim 130$ and $A \sim 160$. See for example Refs. [3, 4, 5, 6, 7]. For 2-qp bands of odd-odd nuclei, signature inversions generally take place in low-spin regions including the bandhead states. For odd- A nuclei, they occur at higher spins than the first backbendings, i.e., in 3-qp bands [8]. Possible mechanisms for signature inversion have been proposed, such as triaxiality [1, 5, 9, 10], band crossing [5, 11], the n-p interaction [8, 12, 13, 14, 15], QQ pairing [16, 17], and the drift of the rotational axis in triaxial nuclei [18].

In $A \sim 160$ mass region, signature inversions have been extensively investigated for the bands based on the configurations $\pi h_{11/2} \otimes \nu i_{13/2}$ and $\pi h_{9/2} \otimes \nu i_{13/2}$. Recently, signature inversions in the odd-odd nucleus ^{174}Re were found not only for the two configurations mentioned above [19] but also for a new band based on the configuration $\pi h_{9/2} \otimes \nu 5/2^-$ [512] [20]. The authors of Ref. [20] suggested that the $\nu 2f_{7/2}$ and $\nu 1h_{9/2}$ configuration admixture may be a possible reason for signature inversion in the band $\pi h_{9/2} \otimes \nu 5/2^-$ [512]. The

investigation of the neighboring odd- N nuclei ^{173}W and ^{175}Os would be beneficial to the interpretation thereof. A recent experiment on ^{173}W was performed [21] and three former observed rotational bands [22], whose configurations are respectively proposed as $\nu 5/2^-$ [512], $\nu 7/2^+$ [633] and $\nu 1/2^-$ [521], were extended to higher spin states. It is interesting to note that signature inversion for band $\nu 5/2^-$ [512] is observed at spin $\frac{35}{2}\hbar$. Signature inversion in band $\nu 5/2^-$ [512] is also observed in other isotones of ^{173}W , i.e., ^{171}Hf [23] and ^{175}Os [24].

The aim of the present work is to investigate signature splitting in ^{173}W in the triaxial particle rotor model. The band $\nu 7/2^+$ [633] in ^{173}W and similar bands in ^{175}W have been investigated by assuming a quasi-particle in a deformed Nilsson potential coupled with an axial symmetric rotor [22]. In this paper, the effect of triaxiality will be investigated. The model will be briefly introduced in Sec. II. Signature splitting of bands $\nu 5/2^-$ [512] and $\nu 7/2^+$ [633] will be discussed in detail in Sec. III and a brief summary will be given in Sec. IV.

II. FORMALISM

The particle rotor model (PRM) adopted here is same as in Refs. [25, 26] and has been extensively used in the investigation of the chirality in atomic nuclei [27, 28, 29, 30]. The model Hamiltonian can be expressed as,

$$H = H_{\text{coll}} + H_{\text{intr}}. \quad (1)$$

The collective Hamiltonian with a triaxial rotor can be written as

$$H_{\text{coll}} = \sum_{i=1}^3 \frac{\hat{R}_i^2}{2\mathcal{J}_i} = \sum_{i=1}^3 \frac{(\hat{I}_i - \hat{j}_i)}{2\mathcal{J}_i}, \quad (2)$$

where $\hat{R}_i, \hat{I}_i, \hat{j}_i$ respectively denote the angular momentum operators for the core, nucleus, as well as the valence nucleon. The moments of inertia for irrotational flow are given by

$$\mathcal{J}_i = \frac{4}{3} \mathcal{J}_0 \sin^2(\gamma - \frac{2\pi}{3}i), \quad (i = 1, 2, 3), \quad (3)$$

where \mathcal{J}_0 depends on the quadrupole deformation ε_2 and the nuclear mass A [31], while γ denotes the degree of triaxiality.

The intrinsic Hamiltonian for valence nucleon is

$$H_{\text{intr}} = H_{\text{sp}} + H_{\text{pair}} = \sum_{\nu>0} (\varepsilon_\nu - \lambda)(a_\nu^+ a_\nu + a_{\bar{\nu}}^+ a_{\bar{\nu}}) - \frac{\Delta}{2} \sum_{\nu>0} (a_\nu^+ a_{\bar{\nu}}^+ + a_{\bar{\nu}} a_\nu), \quad (4)$$

where λ denotes the Fermi energy, Δ the pairing gap parameter, and $|\bar{\nu}\rangle$ the time-reversal state of $|\nu\rangle$. The single particle states $|\nu\rangle$ and corresponding energies ε_ν are obtained by diagonalizing the Hamiltonian H_{sp} . Similar to Refs. [32, 33], we employ the Nilsson type Hamiltonian,

$$H_{\text{sp}} = \left(\frac{p^2}{2m} + \frac{1}{2}m\omega_0^2\rho^2 \right) - \frac{2}{3}\varepsilon_2\sqrt{\frac{4\pi}{5}}\hbar\omega_0\rho^2 \left[\cos\gamma Y_{20} + \frac{1}{\sqrt{2}}\sin\gamma(Y_{22} + Y_{2-2}) \right] - \kappa\hbar\omega_0 \{ 2\vec{l} \cdot \vec{s} + \mu(\vec{l}^2 - \langle \vec{l}^2 \rangle_N) \}. \quad (5)$$

The single particle states are thus written as

$$a_\nu^+|0\rangle = \sum_{Nlj\Omega} c_{Nlj\Omega}^{(\nu)}\psi_{j\Omega}^{Nl}, \quad a_{\bar{\nu}}^+|0\rangle = \sum_{Nlj\Omega} (-1)^{j-\Omega}c_{Nlj\Omega}^{(\nu)}\psi_{j-\Omega}^{Nl}, \quad (6)$$

where Ω is the projection of the single-particle angular momentum \hat{j} along the 3-axis and can be restricted to the values $\dots, -7/2, -3/2, +1/2, +5/2, \dots$ due to time-reversal degeneracy [32, 33].

To obtain the PRM solutions, the total Hamiltonian (1) must be diagonalized in a complete basis space, which couples the rotation of the inert core with the intrinsic wave functions of the valence nucleons. When pairing correlations are neglected, one can construct the so-called strong coupling basis as

$$|IMK\nu\rangle = \sqrt{\frac{1}{2}}\sqrt{\frac{2I+1}{8\pi^2}} [D_{M,K}^I a_\nu^+|0\rangle + (-1)^{I-K}D_{M,-K}^I a_{\bar{\nu}}^+|0\rangle] \quad \text{for } K = \dots, -7/2, -3/2, +1/2, +5/2, \dots. \quad (7)$$

The restriction on values of K is due to the fact that the basis states are symmetrized under the point group D_2 , which leads to $K - \Omega$ being an even integer [32]. The matrix elements of the Hamiltonians given by Eqs. (2) and (5), can be evaluated in the basis (7), and thereafter diagonalization yields eigenenergies and eigenstates of the PRM Hamiltonian.

To include pairing effects in the PRM, one should replace the single particle state $a_\nu^+|0\rangle$ in the basis states (7) with the BCS quasiparticle state $\alpha_\nu^+|\tilde{0}\rangle$ to obtain a new expansion basis, where $|\tilde{0}\rangle$ is the BCS vacuum state. The quasiparticle operators α_ν^+ are given by

$$\begin{pmatrix} \alpha_\nu^+ \\ \alpha_{\bar{\nu}} \end{pmatrix} = \begin{pmatrix} u_\nu & -v_\nu \\ v_\nu & u_\nu \end{pmatrix} \begin{pmatrix} a_\nu^+ \\ a_{\bar{\nu}} \end{pmatrix}, \quad (8)$$

where $u_\nu^2 + v_\nu^2 = 1$. In this new basis, the wave functions of the PRM Hamiltonian are written as

$$|IM\rangle = \sum_{K,\nu} C_\nu^{IK} |IMK\nu\rangle, \quad (9)$$

in which ν represents the quasiparticle states $\alpha_\nu^+|\tilde{0}\rangle$ instead of $\alpha_\nu^+|0\rangle$. Furthermore, single-particle energies ε_ν should be replaced by quasiparticle energies $\varepsilon'_\nu = \sqrt{(\varepsilon_\nu - \lambda)^2 + \Delta^2}$. The total Hamiltonian then becomes:

$$H = H_{\text{coll}} + \sum_{\nu} \varepsilon'_\nu (\alpha_\nu^+ \alpha_\nu + \alpha_{\bar{\nu}}^+ \alpha_{\bar{\nu}}). \quad (10)$$

To construct the matrix of the above Hamiltonian, in comparison with the case excluding pairing, each single-particle matrix element needs to be multiplied by a pairing factor $u_\mu u_\nu + v_\mu v_\nu$ [31, 33]. The occupation factor v_ν of the state ν is given by

$$v_\nu^2 = \frac{1}{2} \left[1 - \frac{\varepsilon_\nu - \lambda}{\varepsilon'_\nu} \right]. \quad (11)$$

III. RESULTS AND DISCUSSION

In the present calculations, the values of κ and μ in the Nilsson type Hamiltonian (5) are taken from Ref. [34], i.e., $\kappa = 0.062$ and $\mu = 0.43$ for the main oscillator quantum number $N = 5$, $\kappa = 0.062$ and $\mu = 0.34$ for $N = 6$. The quadrupole deformation parameter ε_2 takes a value of 0.24 according to Ref. [35]. The triaxiality parameter γ is to be adjusted by the signature splitting. An off-diagonal Coriolis attenuation parameter ξ is introduced to reproduce the experimental energy spectra [33], and a variable moment of inertia is used when necessary, $\mathcal{J}_0(I) = \mathcal{J}_0 \sqrt{1 + bI(I+1)}$ [36]. The neutron Fermi energy λ_n is taken to be the energy of the single-particle level occupied by the last neutron. The pairing gap parameter Δ is given by the empirical value of 0.81 MeV.

For the axially deformed case, the orbitals are usually denoted by the Nilsson quantum number $\Omega^\pi [Nn_3\Lambda]$. For the triaxially deformed case, as Ω is not a good quantum number, the number ν is used to denote the single-particle state according to the sequence of the energy. For convenience, the Nilsson quantum number is also used to denote approximately the single particle state in the triaxially deformed case. From the standard Nilsson single particle level diagram, the last neutron of ^{173}W lies in the orbital $1/2^-$ [521] at $\varepsilon_2 = 0.24$, with the orbitals $7/2^+$ [633], $5/2^-$ [512] nearby, which is consistent with the configurations

proposed for the three observed bands [22]. Furthermore, the calculated energy difference between the states $7/2^+[633]$ and $5/2^-[512]$ is 67.6 keV at $\varepsilon_2 = 0.24$, which agrees with the observed bandhead energy difference 85.5 keV in ^{173}W [21].

In Table I, seven positive-parity orbitals and seven negative-parity orbitals near the Fermi level adopted for band $\nu 7/2^+[633]$ at $\gamma = 15^\circ$, and band $\nu 5/2^-[512]$ at $\gamma = 12^\circ$ in the present triaxial PRM calculations are listed. The neutron Fermi energy λ_n is 51.46 MeV for $\gamma = 15^\circ$, and 51.51 MeV for $\gamma = 12^\circ$. The above mentioned orbitals are used to couple with the core in the calculations for the positive-parity and negative-parity bands of ^{173}W respectively. Their approximate Nilsson quantum numbers, single particle energies, and main components expanded in the basis $|Nlj\Omega\rangle$ are also listed. One can see that the main components for the positive parity orbitals near the Fermi level belong to the $i_{13/2}$ sub-shell components, while for the negative-parity band there is a strong mixture of $1h_{9/2}$ and $2f_{7/2}$ sub-shells.

In the following, using the triaxial particle rotor model, we will focus our discussion on signature splitting in the bands $\nu 7/2^+[633]$ and $\nu 5/2^-[512]$.

A. Band $\nu 7/2^+[633]$

The calculated energy spectra $E(I)$, signature splitting $S(I)$ for the band $\nu 7/2^+[633]$ and subsequent comparison with data are illustrated in Fig. 1. Firstly, the moment of inertia \mathcal{J}_0 is adjusted to reproduce the energy spectra by switching off the triaxiality and Coriolis attenuation. As shown in Fig. 1a, where the best fitting by adjusting \mathcal{J}_0 alone is given, the calculation gives the lowest state is at $I = \frac{9}{2}\hbar$ instead of $I = \frac{7}{2}\hbar$. Furthermore, obvious deviations with the data for both the energy spectra and the amplitude of signature splitting can be seen.

Secondly, as in Ref. [33], the Coriolis attenuation $\xi = 0.7$ is introduced as shown in Fig. 1b. The calculation with Coriolis attenuation can give correctly the lowest state at $I = \frac{7}{2}\hbar$ and achieve better agreement with the energy in almost whole spin region. However, the amplitude of signature splitting is too small to reproduce the data.

With the triaxiality deformation switched on and the corresponding Fermi energy altered as the energy of the level occupied by the last neutron, good agreement with the amplitude of signature splitting is achieved, as shown in Fig. 1c. It is interesting to note that the triaxiality improves the amplitude of the signature splitting while does not ruin the agreement with

the energy in the whole spin region.

From Figs. 1a - 1c, the important roles of the Coriolis attenuation and γ degree of freedom are shown explicitly to reproduce the energy spectra $E(I)$ and signature splitting $S(I)$ for the band $\nu 7/2^+[633]$. A further check was done and it is confirmed that by adjusting the γ alone without the Coriolis attenuation, the energy spectra $E(I)$ for the whole spin region cannot be reproduced.

In Ref. [22], the signature splitting for the band $\nu 7/2^+[633]$ has been reproduced without involving triaxiality. To clarify this point the calculations with the same parameters as in Ref. [22] are performed and the results are shown in Fig. 2. If the Coriolis attenuation is taken into account for the off-diagonal Coriolis matrix elements for all K, K' , good agreement with the energy can be achieved but not the amplitude of signature splitting, as shown in Fig. 2a. In order to reproduce both the energy and the amplitude of signature splitting without triaxiality, in Ref. [22], the Coriolis attenuation has to be taken only for the matrix elements associated with the single-quasiparticle state (i.e., K or $K' = 7/2$), as shown in Fig. 2b.

To show the influence of the triaxiality parameters on the electromagnetic properties in the band $\nu 7/2^+[633]$, the calculated $B(M1)$, $B(E2)$ and $B(M1)/B(E2)$ values are illustrated and compared with the data available in Fig. 3. The formulas for $B(M1)$ and $B(E2)$ are the same as in Refs. [29, 31]. In the calculations, the empirical intrinsic quadrupole moment $Q_0 = 6$ eb, the collective gyromagnetic factor $g_R = 0.43$, and the gyromagnetic factor of quasineutron $g_n = g_l \pm (g_s - g_l)/(2l + 1)$ with $g_l = 0, g_s = -2.68$ have been adopted. The calculated $B(M1)$ values exhibit a staggering. Just as $S(I)$, the amplitudes of the $B(M1)$ staggering are larger for $\gamma = 15^\circ$ than that for $\gamma = 0^\circ$. While the $B(E2)$ values for triaxial deformed case are suppressed in comparison with the axial deformed case. Therefore, the calculated $B(M1)/B(E2)$ staggering for this band can be enhanced obviously by introducing triaxiality. The calculated $B(M1)/B(E2)$ staggerings with triaxiality achieve better agreement with the data available [22] than the ones without triaxiality.

We also investigate the main components of the wave functions for spins $I = \frac{7}{2}, \frac{9}{2}, \frac{23}{2}, \frac{25}{2}, \frac{39}{2}, \frac{41}{2}\hbar$ in band $\nu 7/2^+[633]$, which are listed in Table II. The orbital $|4\rangle$, i.e., $7/2^+[633]$ in Table I, is the dominant component at the bandhead with $\sum_K |C_4^{IK}|^2 \sim 75\%$. As the nucleus rotates faster, due to the large Coriolis matrix elements of $i_{13/2}$ sub-shell, at $I = \frac{41}{2}$, the contribution of the orbital $|4\rangle$ is decreased to $\sim 21\%$.

B. Band $\nu 5/2^-$ [512]

The energy spectra $E(I)$ and signature splitting $S(I)$ for the band $\nu 5/2^-$ [512] calculated by the PRM are given in Fig. 4 and compared with data [21]. In the calculations, $\varepsilon_2 = 0.24$, and $\mathcal{J}_0 = 35 \text{ MeV}^{-1} \hbar^2$. The pairing parameter $\Delta_n = 0.81 \text{ MeV}$. The Fermi energy λ_n , triaxial deformation parameter γ , Coriolis attenuation factor ξ and the parameter b in the variable moment of inertia in the panels are respectively, (a) $\lambda_n = 51.41 \text{ MeV}$, $\gamma = 0^\circ$, $\xi = 1.0$ and $b = 0$; (b) $\lambda_n = 51.41 \text{ MeV}$, $\gamma = 0^\circ$, $\xi = 0.7$ and $b = 0$; (c) $\lambda_n = 51.41 \text{ MeV}$, $\gamma = 0^\circ$, $\xi = 0.7$ and $b = 0.002$; (d) $\lambda_n = 51.51 \text{ MeV}$, $\gamma = 12^\circ$, $\xi = 0.7$ and $b = 0.002$.

Using a constant moment of inertia, the calculated energy can only agree with data in the lower spin region as shown in Fig. 4a. As shown in Fig. 4b, compared with the band $\nu 7/2^+$ [633], the Coriolis attenuation has less influence for the band $\nu 5/2^-$ [512] due to the low j components ($\frac{7}{2}$ and $\frac{9}{2}$). To reproduce the observed energy spectra $E(I)$, a variable moment of inertia is necessary, as shown in Fig. 4c.

Similar to the band $\nu 7/2^+$ [633], without the γ degree of freedom, the calculated amplitudes of signature splitting $S(I)$ are small compared with the observed ones. As shown in Fig. 4d, after introducing the triaxiality ($\gamma = 12^\circ$), signature splitting $S(I)$ for $I < \frac{35}{2} \hbar$ is reproduced perfectly. Without invoking the triaxiality, systematic calculations by simply adjusting all the other parameters, including ε_2 and Δ , have been done and it is found that the spectra $E(I)$ and the signature splitting $S(I)$ can not be reproduced simultaneously for band $\nu 5/2^-$ [512], which shows the necessary of triaxial deformation for this band.

Although signature splitting $S(I)$ for $I < \frac{35}{2} \hbar$ can be well reproduced by introducing triaxiality, the calculated signature splitting $S(I)$ for $I \geq \frac{35}{2} \hbar$ is inconsistent with the data. In particular, there is a signature inversion at spin $\frac{35}{2} \hbar$, i.e., $S(I)$ is smaller for $I = 2n + 1/2$ ($\alpha = +1/2$) for $I < \frac{35}{2} \hbar$ and for $I = 2n - 1/2$ ($\alpha = -1/2$) for $I \geq \frac{35}{2} \hbar$, which cannot be reproduced by the present calculation.

The main components of the wave functions for spins $I = \frac{5}{2}, \frac{7}{2}, \frac{23}{2}, \frac{25}{2}, \frac{39}{2}, \frac{41}{2} \hbar$ in band $\nu 5/2^-$ [512] are listed in Table III to examine the evolution of the wave function. The orbital $|3\rangle$, i.e., $5/2^-$ [512] in Table I, is the dominant component at the bandhead with $\sum_K |C_3^{IK}|^2 \sim 96\%$. As the nucleus rotates faster, at $I = \frac{41}{2}$, the contribution of the orbital $|3\rangle$ is decreased to $\sim 40\%$. As given in Table I, both orbitals $2f_{7/2}$ and $1h_{9/2}$ contribute significantly to the orbital $|3\rangle$, i.e., $5/2^-$ [512]. As the orbital $2f_{7/2}$ contributes $\sim 64\%$ and

the orbital $1h_{9/2} \sim 25\%$ to the orbital $|3\rangle$, we attempt to understand Fig. 4d in terms of the orbitals $2f_{7/2}$ and $1h_{9/2}$ in the following.

For the band with one quasiparticle in a high- j orbital, the favored signature can be obtained by $\alpha_f = (-1)^{j-1/2}1/2$ [2], i.e., $\alpha_f = -1/2$ for orbital $2f_{7/2}$ and $\alpha_f = +1/2$ for orbital $1h_{9/2}$. This is consistent with the calculated results in Fig. 5, in which the signature splitting $S(I)$ in PRM calculations with the valence neutron in $2f_{7/2}$ single- j shell (upper panel), $1h_{9/2}$ single- j shell (middle panel) and their mixture (lower panel) are given in comparison with the data for the band $\nu 5/2^-$ [512] in ^{173}W [21]. In the calculations, $\varepsilon_2 = 0.24$, $\gamma = 12^\circ$, $\mathcal{J}_0 = 35 \text{ MeV}^{-1}\hbar^2$, $b = 0.002$, $\xi = 1.0$, $\Delta_n = 0.81 \text{ MeV}$, and λ_n is taken to be the energy of the level $\Omega = \frac{5}{2}$ in the corresponding single- j shell.

For $I < \frac{35}{2}\hbar$, the observed phase of $S(I)$ in band $\nu 5/2^-$ [512] is consistent with that for $1h_{9/2}$ configuration, but different from that for $2f_{7/2}$. For $I \geq \frac{35}{2}\hbar$, the observed phase of $S(I)$ are no longer consistent with that for $1h_{9/2}$, but consistent with that for $2f_{7/2}$. As the amplitudes of $S(I)$ are concerned, the amplitudes of $S(I)$ for $1h_{9/2}$ are larger than those for $2f_{7/2}$ and both of them are much larger than the observed ones. Therefore, although the orbital $2f_{7/2}$ is the predominant component in the observed band $\nu 5/2^-$ [512], the strong competition from $1h_{9/2}$ results in signature splitting $S(I)$ for the $I < \frac{35}{2}\hbar$ as shown in Fig. 4d.

As for signature inversion at $I = \frac{35}{2}\hbar$, one straightforward explanation may be attributed to the superiority of the orbital $2f_{7/2}$ over $1h_{9/2}$ after $I > \frac{35}{2}\hbar$. By mixing the energy spectra according to the mixing ratios of $2f_{7/2}$ and $1h_{9/2}$ in orbital $\nu 5/2^-$ [512] in Table. I, the $S(I)$ is extracted and compared with the observed one in band $\nu 5/2^-$ [512] in the lower panel in Fig. 5. It is interesting to note that the observed phase of $S(I)$ and signature inversion in band $\nu 5/2^-$ [512] can be perfectly reproduced although the deficiencies still exist for the amplitude. We also note that there is an upbending for this band around $I = \frac{35}{2}\hbar$ based on the analysis of spin alignment and the moment of inertia. However, a self-consistent description of the upbending and signature inversion is beyond the scope of the present one quasiparticle PRM.

IV. CONCLUSION

A particle rotor model with a quasi-neutron coupled with a triaxial rotor is applied to study signature splitting of the bands built on the intruder orbital $\nu 7/2^+$ [633] and non-

intruder orbital $\nu 5/2^-$ [512] in ^{173}W . With triaxiality and Coriolis attenuation, the correct spin of the lowest state, energy spectra $E(I)$ and signature splitting $S(I)$ for the band $\nu 7/2^+$ [633] are well reproduced.

The phase and amplitude of signature splitting in the band of the non-intruder orbital $\nu 5/2^-$ [512] is attributed to the strong competition of the contribution from its main components $2f_{7/2}$ and $1h_{9/2}$. Similar competitions should take important roles in bands with other non-intruder orbitals, and the conclusion is also helpful to interpret the signature splitting in the neighbor odd-odd nuclei, such as the band $\pi h_{9/2} \otimes \nu 5/2^-$ [512] in ^{174}Re [20]. Although triaxiality ($\gamma = 12^\circ$) can reproduce signature splitting $S(I)$ for $I < \frac{35}{2}\hbar$ and energy spectra $E(I)$ perfectly, signature inversion for $I = \frac{35}{2}\hbar$ in band $\nu 5/2^-$ [512] still cannot be understood by the triaxiality, Coriolis attenuation, and variability of the moment of inertia. As an upbending happens, a proper description of signature inversion self-consistently is beyond the scope of the present one quasiparticle PRM.

Acknowledgments

Helpful discussions with G.C. Hillhouse, Y.H. Zhang and X.H. Zhou are gratefully acknowledged. This work is partly supported by Major State Basic Research Developing Program 2007CB815000, the National Natural Science Foundation of China under Grant Nos. 10505002, 10435010, 10605001, 10775004 and 10221003.

-
- [1] R. Bengtsson, H. Frisk, F. R. May and J. A. Pinston, Nucl. Phys. **A415**, 189 (1984).
 - [2] F. S. Stephens, Rev. Mod. Phys. **47**, 43 (1975).
 - [3] Y. Liu, Y. Ma, H. Yang, and S. Zhou, Phys. Rev. C **52**, 2514 (1995).
 - [4] Y. Liu, J. Lu, Y. Ma, S. Zhou, and H. Zheng, Phys. Rev. C **54**, 719 (1996).
 - [5] C. Plettner *et al.*, Phys. Rev. Lett. **85**, 2454 (2000).
 - [6] G. García Bermúdez and M. A. Cardona, Phys. Rev. C **64**, 034311 (2001).
 - [7] S. Singh, S. S. Malik and A. K. Jain, Phys. Rev. C **75**, 067301 (2007).
 - [8] N. Tajima, Nuc. Phys. **A572**, 365 (1994).
 - [9] A. Ikeda and T. Shimano, Phys. Rev. Lett. **63**, 139 (1989).

- [10] I. Hamamoto and B. Mottelson, Phys. Lett. **B132**, 7 (1983).
- [11] K. Hara and Y. Sun, Nucl. Phys. **A537**, 77 (1992).
- [12] I. Hamamoto, Phys. Lett. **B179**, 327 (1986).
- [13] P. B. Semmes, and I. Ragnarsson, Proc. of Int. Conf. on High-Spin Phys. and Gamma-Soft Nuclei, Pittsburgh, 1990, World Scientific, Singapore, (1991) P.500.
- [14] B. Cederwall *et al.*, Nucl. Phys. **A542**, 454 (1992).
- [15] R. Zheng, S. Zhu, N. Cheng, and J. Wen, Phys. Rev. C **64**, 014313 (2001).
- [16] W. Satuła and R. Wyss, Acta Phys. Pol. **B27**, 121 (1996).
- [17] F. R. Xu, W. Satuła, and R. Wyss, Nucl. Phys. **A669**, 119 (2000).
- [18] Z. C. Gao, Y. S. Chen, and Y. Sun, Phys. Lett. **B634**, 195 (2006).
- [19] Y. H. Zhang *et al.*, Chin. Phys. Lett. **22**, 2788 (2005).
- [20] Y. H. Zhang *et al.*, Chin. Phys. Lett. **24**, 1203 (2007).
- [21] Y. H. Zhang (private communication).
- [22] P. M. Walker, G. D. Dracoulis, A. Johnston, J. R. Leigh, M. G. Slocombe and I. F. Wright, J. Phys. **G4**, 1655 (1978).
- [23] D. M. Cullen *et al.*, Nucl. Phys. **A673**, 3 (2000).
- [24] B. Fabricius, G. D. Dracoulis, R. A. Bark, A. E. Stuchbery, T. Kibèdi and A. M. Baxter, Nucl. Phys. **A511**, 345 (1990).
- [25] S. Frauendorf and J. Meng, Z. Phys. **A365**, 263 (1996).
- [26] S. Frauendorf and J. Meng, Nucl. Phys. **A617**, 131 (1997).
- [27] J. Peng, J. Meng, S. Q. Zhang, Phys. Rev. C **68**, 044324 (2003).
- [28] S. Y. Wang, S. Q. Zhang, B. Qi, and J. Meng, Phys. Rev. C **75**, 024309 (2007).
- [29] S. Q. Zhang, B. Qi, S. Y. Wang, and J. Meng, Phys. Rev. C **75**, 044307(2007).
- [30] S.Y. Wang, S.Q. Zhang, B.Qi, J. Peng, J. M. Yao, J. Meng, Phys. Rev. C **77**, 034314 (2008).
- [31] J. Meyer-ter-vehn, Nucl. Phys. **A249**, 111 (1975).
- [32] S. E. Larsson, G. Leander and I. Ragnarsson, Nucl. Phys. **A307**, 189 (1978).
- [33] I. Ragnarsson and P. B. Semmes, Hyperfine Interaction **43**, 425 (1988).
- [34] T. Bengtsson and I. Ragnarsson, Nucl. Phys. **A436**, 14 (1985).
- [35] P. Möller, J. R. Nix, W. D. Myers and W. J. Swiatecki, At. Data Nucl. Data Tables **59**, 185 (1995).
- [36] C. S. Wu and J. Y. Zeng, Commu. Theor. Phys. **8**, 51 (1987).

TABLE I: Positive and negative single-particle levels $|\nu\rangle$ adopted for the band $\nu 7/2^+[633]$ at $\gamma = 15^\circ$, and the band $\nu 5/2^- [512]$ at $\gamma = 12^\circ$ for the present triaxial PRM calculations. The approximate Nilsson quantum numbers, single particle energies, and main components expanded in the basis $|Nlj\Omega\rangle$ are shown. The neutron Fermi energy λ_n is 51.46 MeV for $\gamma = 15^\circ$, and 51.51 MeV for $\gamma = 12^\circ$.

γ	$ \nu\rangle$	$\Omega^\pi[Nn_z\Lambda]$	ε_ν (MeV)	Main components in terms of $ Nlj\Omega\rangle$
15°	1)	$1/2^+[660]$	49.32	$0.784 6i_{13/2} \frac{1}{2}\rangle + 0.423 6i_{13/2} -\frac{3}{2}\rangle + 0.353 6g_{9/2} \frac{1}{2}\rangle$
	2)	$3/2^+[651]$	50.16	$0.798 6i_{13/2} -\frac{3}{2}\rangle - 0.360 6i_{13/2} \frac{1}{2}\rangle + 0.337 6g_{9/2} -\frac{3}{2}\rangle$
	3)	$5/2^+[642]$	50.90	$0.903 6i_{13/2} \frac{5}{2}\rangle - 0.292 6g_{9/2} \frac{5}{2}\rangle + 0.182 6g_{9/2} \frac{1}{2}\rangle$
	4)	$7/2^+[633]$	51.95	$0.951 6i_{13/2} -\frac{7}{2}\rangle + 0.214 6g_{9/2} -\frac{7}{2}\rangle - 0.159 6g_{9/2} -\frac{3}{2}\rangle$
	5)	$9/2^+[624]$	53.26	$0.973 6i_{13/2} \frac{9}{2}\rangle + 0.157 6g_{9/2} \frac{5}{2}\rangle - 0.124 6g_{9/2} \frac{9}{2}\rangle$
	6)	$1/2^+[651]$	53.85	$0.566 6g_{9/2} \frac{1}{2}\rangle - 0.531 6d_{5/2} \frac{1}{2}\rangle - 0.238 6s_{1/2} \frac{1}{2}\rangle$
	7)	$11/2^+[615]$	54.76	$0.985 6i_{13/2} -\frac{11}{2}\rangle - 0.156 6g_{9/2} -\frac{7}{2}\rangle + 0.060 6i_{11/2} -\frac{11}{2}\rangle$
12°	1)	$3/2^- [521]$	49.78	$0.670 5f_{7/2} -\frac{3}{2}\rangle - 0.592 5h_{9/2} -\frac{3}{2}\rangle + 0.221 5p_{3/2} -\frac{3}{2}\rangle$
	2)	$5/2^- [523]$	50.26	$0.814 5h_{9/2} \frac{5}{2}\rangle - 0.394 5f_{7/2} \frac{5}{2}\rangle + 0.227 5f_{5/2} \frac{5}{2}\rangle$
	3)	$5/2^- [512]$	51.51	$0.798 5f_{7/2} \frac{5}{2}\rangle + 0.495 5h_{9/2} \frac{5}{2}\rangle - 0.213 5p_{3/2} \frac{1}{2}\rangle$
	4)	$1/2^- [521]$	51.63	$0.465 5p_{1/2} \frac{1}{2}\rangle + 0.457 5f_{7/2} \frac{1}{2}\rangle - 0.442 5h_{9/2} \frac{1}{2}\rangle$
	5)	$7/2^- [514]$	52.08	$0.922 5h_{9/2} -\frac{7}{2}\rangle + 0.274 5f_{7/2} -\frac{7}{2}\rangle - 0.195 5f_{5/2} -\frac{3}{2}\rangle$
	6)	$7/2^- [503]$	53.50	$0.841 5f_{7/2} -\frac{7}{2}\rangle - 0.340 5h_{9/2} -\frac{7}{2}\rangle - 0.264 5p_{3/2} -\frac{3}{2}\rangle$
	7)	$1/2^- [510]$	53.56	$0.500 5f_{5/2} -\frac{3}{2}\rangle - 0.468 5p_{3/2} \frac{1}{2}\rangle - 0.406 5f_{5/2} \frac{1}{2}\rangle$

TABLE II: The main components expanded in the strong coupling basis $|IMK\nu\rangle$ in Eq.(7) (denoted as $|K\nu\rangle$ for short) for selected states in the band $\nu 7/2^+[633]$. The parameters in the calculations are the same as in Fig. 1c.

I^π	Main components in terms of $ K\nu\rangle$
$\frac{7}{2}^+$	$0.868 -\frac{7}{2} 4\rangle + 0.485 \frac{5}{2} 3\rangle - 0.094 -\frac{3}{2} 2\rangle - 0.019 -\frac{3}{2} 3\rangle$
$\frac{9}{2}^+$	$0.806 -\frac{7}{2} 4\rangle - 0.554 \frac{5}{2} 3\rangle + 0.143 -\frac{3}{2} 2\rangle - 0.113 \frac{9}{2} 5\rangle$
...	...
$\frac{23}{2}^+$	$0.652 -\frac{7}{2} 4\rangle + 0.582 \frac{5}{2} 3\rangle + 0.232 -\frac{3}{2} 2\rangle + 0.224 \frac{9}{2} 5\rangle$
$\frac{25}{2}^+$	$0.558 \frac{5}{2} 3\rangle - 0.500 -\frac{7}{2} 4\rangle - 0.371 -\frac{3}{2} 2\rangle - 0.283 \frac{1}{2} 3\rangle$
...	...
$\frac{39}{2}^+$	$0.524 -\frac{7}{2} 4\rangle - 0.474 \frac{5}{2} 3\rangle - 0.263 \frac{9}{2} 3\rangle - 0.256 -\frac{3}{2} 4\rangle$
$\frac{41}{2}^+$	$0.465 \frac{5}{2} 3\rangle - 0.418 -\frac{3}{2} 2\rangle - 0.340 -\frac{7}{2} 4\rangle - 0.334 \frac{1}{2} 3\rangle$
...	...

TABLE III: Same as Table. II, but for selected states in the band $\nu 5/2^- [512]$ and the parameters in the calculations are the same as Fig. 4d.

I^π	Main components in terms of $ K\nu\rangle$
$\frac{5}{2}^-$	$0.982 \frac{5}{2} 3\rangle - 0.111 \frac{5}{2} 4\rangle + 0.088 -\frac{3}{2} 1\rangle - 0.078 -\frac{3}{2} 4\rangle$
$\frac{7}{2}^-$	$0.926 \frac{5}{2} 3\rangle + 0.313 -\frac{7}{2} 5\rangle - 0.126 -\frac{3}{2} 1\rangle + 0.074 \frac{5}{2} 4\rangle$
...	...
$\frac{23}{2}^-$	$0.669 \frac{5}{2} 3\rangle + 0.487 -\frac{7}{2} 5\rangle - 0.228 \frac{9}{2} 3\rangle - 0.207 \frac{1}{2} 3\rangle$
$\frac{25}{2}^-$	$0.583 \frac{5}{2} 3\rangle - 0.464 -\frac{7}{2} 5\rangle - 0.231 \frac{1}{2} 3\rangle - 0.219 \frac{9}{2} 3\rangle$
...	...
$\frac{39}{2}^-$	$0.532 \frac{5}{2} 3\rangle + 0.408 -\frac{7}{2} 5\rangle - 0.326 \frac{9}{2} 3\rangle - 0.301 \frac{1}{2} 3\rangle$
$\frac{41}{2}^-$	$0.449 \frac{5}{2} 3\rangle - 0.374 -\frac{7}{2} 5\rangle - 0.277 \frac{1}{2} 3\rangle - 0.276 \frac{9}{2} 3\rangle$
...	...

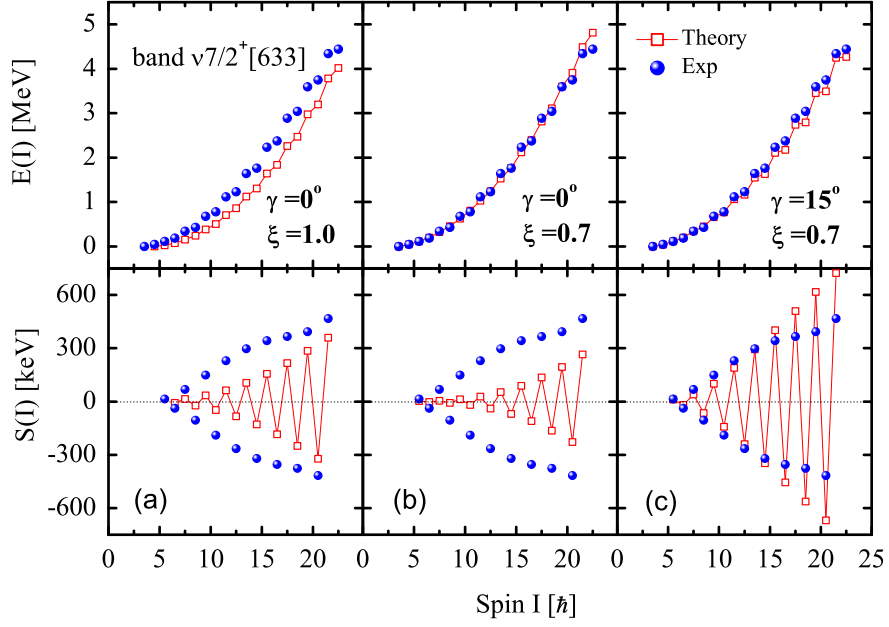


FIG. 1: (color online) The energy spectra $E(I)$ and signature splitting $S(I)$ for the band $\nu 7/2^+ [633]$ in ^{173}W based on the PRM (red squares) in comparison with the data (blue points) [21]. In the calculations, $\varepsilon_2 = 0.24$, $\mathcal{J}_0 = 40 \text{ MeV}^{-1} \hbar^2$ and $b = 0$. The pairing parameter $\Delta_n = 0.81 \text{ MeV}$. The Fermi energy λ_n , triaxial deformation parameter γ and the Coriolis attenuation factor ξ in the left (a), middle (b) and right (c) panels are respectively, $\lambda_n = 51.41 \text{ MeV}$, $\gamma = 0^\circ$, and $\xi = 1.0$ (a); $\lambda_n = 51.41 \text{ MeV}$, $\gamma = 0^\circ$, and $\xi = 0.7$ (b); $\lambda_n = 51.46 \text{ MeV}$, $\gamma = 15^\circ$ and $\xi = 0.7$ (c).

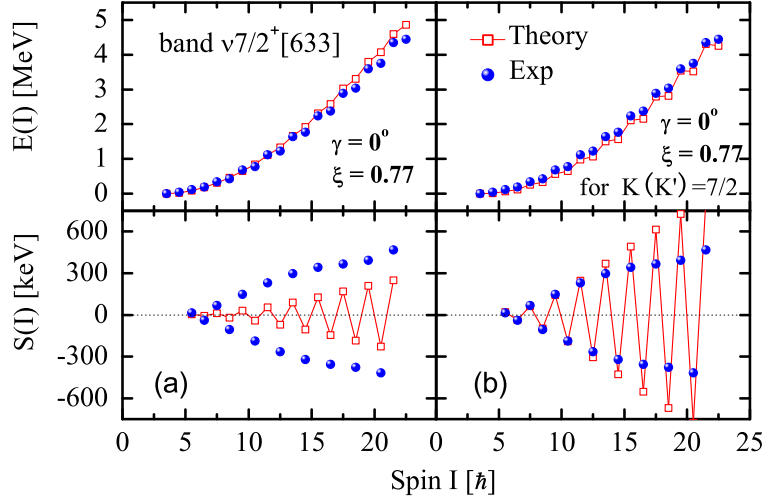


FIG. 2: (color online) The energy spectra $E(I)$ and signature splitting $S(I)$ for the band $\nu 7/2^+ [633]$ in ^{173}W based on the PRM (red squares) without triaxiality in comparison with the data (blue points) [21]. In the calculations, the same as Fig. 9 in Ref. [22], we have chosen $\varepsilon_2 = 0.23$, $\gamma = 0^\circ$, and $\hbar^2/2\mathcal{J} = A_1 + A_2[I(I+1) - K^2]$ with $A_1 = 17.0$ keV and $A_2 = -6.7$ eV. In the left panels (a), the attenuation factor $\xi = 0.77$ is introduced for the off-diagonal Coriolis matrix elements for all K, K' ; while in the right panels (b), the attenuation factor $\xi = 0.77$ is introduced only for the matrix elements associated with the lowest single-quasiparticle state (i.e., K or $K' = 7/2$), the same as in Ref. [22].

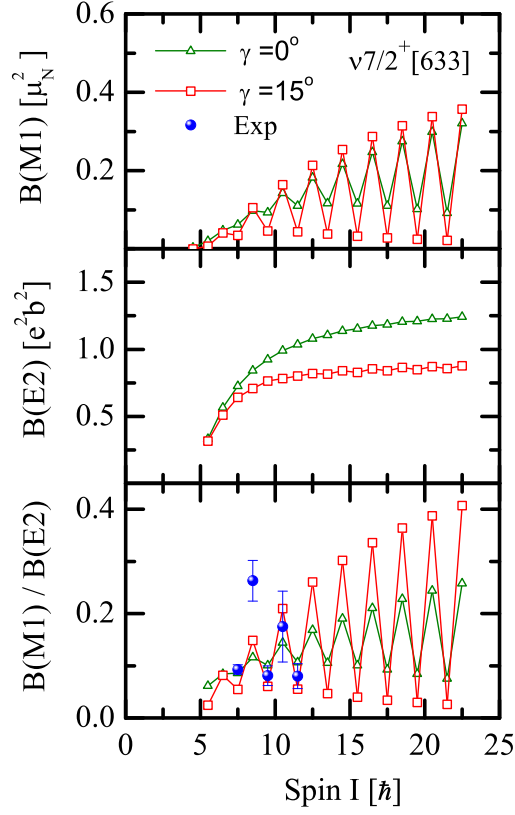


FIG. 3: (color online) $B(M1)$, $B(E2)$ and $B(M1)/B(E2)$ values for the band $\nu 7/2^+[633]$ in ^{173}W based on the PRM with $\gamma = 0^\circ$ (olive triangles) and $\gamma = 15^\circ$ (red squares) in comparison with the available data (blue points) [22]. Other parameters are the same as Fig. 1b and Fig. 1c. In the calculation of electromagnetic transitions, the empirical intrinsic quadrupole moment $Q_0 = 6$ eb, the collective gyromagnetic factor $g_R = 0.43$, and the gyromagnetic factor of quasineutron $g_n = g_l \pm (g_s - g_l)/(2l + 1)$ with $g_l = 0, g_s = -2.68$ have been adopted.

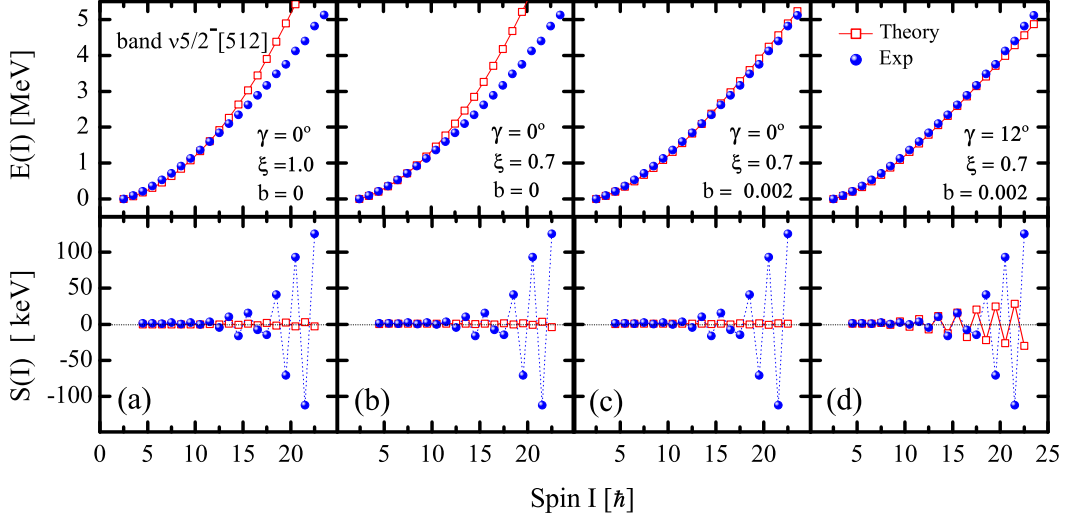


FIG. 4: (color online) The energy spectra $E(I)$ and signature splitting $S(I)$ for the band $\nu 5/2^- [512]$ in ^{173}W based on the PRM (red squares) in comparison with the data (blue points) [21]. In the calculations, $\varepsilon_2 = 0.24$, and $\mathcal{J}_0 = 35 \text{ MeV}^{-1}\hbar^2$. The pairing parameter $\Delta_n = 0.81 \text{ MeV}$. The Fermi energy λ_n , triaxial deformation parameter γ , Coriolis attenuation factor ξ and the parameter b in the variable moment of inertia in the panels are respectively, (a) $\lambda_n = 51.41 \text{ MeV}$, $\gamma = 0^\circ$, $\xi = 1.0$ and $b = 0$; (b) $\lambda_n = 51.41 \text{ MeV}$, $\gamma = 0^\circ$, $\xi = 0.7$ and $b = 0$; (c) $\lambda_n = 51.41 \text{ MeV}$, $\gamma = 0^\circ$, $\xi = 0.7$ and $b = 0.002$; (d) $\lambda_n = 51.51 \text{ MeV}$, $\gamma = 12^\circ$, $\xi = 0.7$ and $b = 0.002$.

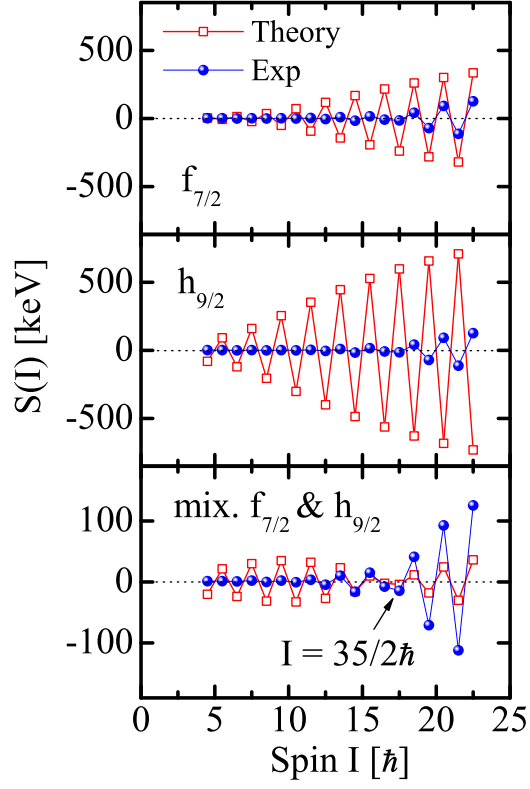


FIG. 5: (color online) Signature splitting $S(I)$ in PRM calculations (red squares) with the valence neutron in $2f_{7/2}$ single- j shell (upper panel), $1h_{9/2}$ single- j shell (middle panel) and their mixture (lower panel) in comparison with the data (blue points) for the band $\nu 5/2^- [512]$ in ^{173}W [21]. In the calculations, $\varepsilon_2 = 0.24$, $\gamma = 12^\circ$, $\mathcal{J}_0 = 35 \text{ MeV}^{-1}\hbar^2$, $b = 0.002$, $\xi = 1.0$, $\Delta_n = 0.81 \text{ MeV}$, and λ_n is taken to be the energy of the level $\Omega = \frac{5}{2}$ in the corresponding single- j shell.